JOURNAL OF Materials CHEMISTRY

Neutron diffraction study of stoichiometric spinel $Li_{1+x}Mn_{2-x}O_4$ showing octahedral 16*c*-site Li-occupation

Helena Berg,*[a] Erik M. Kelder[b] and John O. Thomas[a]

[a]*Inorganic Chemistry, Ångström Laboratory, Uppsala University, Box 538, SE-751 21 Uppsala, Sweden*
[b]*Delft University of Technology, Julianalaan 136, 2628 BL Delft, The Netherlands*

Received 25th June 1998, Accepted 19th October 1998

Stoichiometric $Li_{1+x}Mn_{2-x}O_4$ has been synthesised from $LiOH{\cdot}H_2O$ and manganese(III) acetate. The structure of the compound so formed ($Li_{1+x}Mn_{2-x}O_4$, $x=0.14$) has been refined from neutron powder diffraction data. The sample contained an impurity phase of *ca.* 5 wt% Li_2MnO_3. Under these conditions, two-phase Rietveld refinement showed lithium ions to occupy both tetrahedral 8*a*-sites (100% occupancy) and octahedral 16*c*-sites (7.0% occupancy); this 16*c*-site occupation has not been observed previously. Manganese ions occupy octahedral 16*d*-sites (93.0% occupancy).

Introduction

One of the more interesting cathode materials for rechargeable lithium-ion and lithium-polymer battery applications is $LiMn_2O_4$;[1–6] it is both cheaper and has environmental advantages over $LiCoO_2$, $LiNiO_2$ and V_6O_{13}. $LiMn_2O_4$ has the spinel structure (space group: *Fd*3*m*) with the general formula AB_2O_4, where A and B are cations occupying tetrahedral (8*a*) and octahedral (16*d*) sites, respectively, in an intervening cubic close-packed array of oxygen atoms (32*e* sites). The coordination around the cations is shown in Fig. 1. The interstitial space in the B_2O_4 framework can be seen as a network of tetrahedral 8*a*-sites and octahedral 16*c*-sites, which can function as pathways for the transport of lithium ions in the structure.

$LiMn_2O_4$ is electrochemically active; lithium ions can be extracted, ultimately forming λ-MnO_2,[7] and re-inserted with maintained cubic symmetry. The host structure contracts and expands isotropically during lithium extraction/insertion. $LiMn_2O_4$ undergoes a cubic-to-tetragonal phase transition as more lithium is inserted into the structure to approach $Li_2Mn_2O_4$ (with the mean Mn oxidation state shifting from +3.5 to +3.0). This phase transition coincides with a Jahn–Teller distortion associated with high-spin Mn^{3+} ions, in which the Mn coordination undergoes a cubic-to-tetragonal point-symmetry transition. The theoretical capacity of $LiMn_2O_4$ is 148 mAh g^{-1}, although this figure is never fully achieved. Various attempts have been made to reach this theoretical capacity; particularly through reduction of the Jahn–Teller effect by increasing the mean Mn valency through substitution with some lower-valent ion. Lithium-ion substitution can clearly serve this purpose; this leads to a solid solution of composition $Li_{1+x}Mn_{2-x}O_4$ with $0 \le x \le 0.33$. In practise, this excess lithium has been shown to reduce the capacity of the spinel according to the approximate expression $148(1-3x)$ mAh g^{-1}.[8]

The crystal structure of the cubic lithium-rich spinel, $Li_{1+x}Mn_{2-x}O_4$ has here been determined from neutron powder diffraction data for a sample containing a Li_2MnO_3 impurity phase (space group: *C*2/*m*).

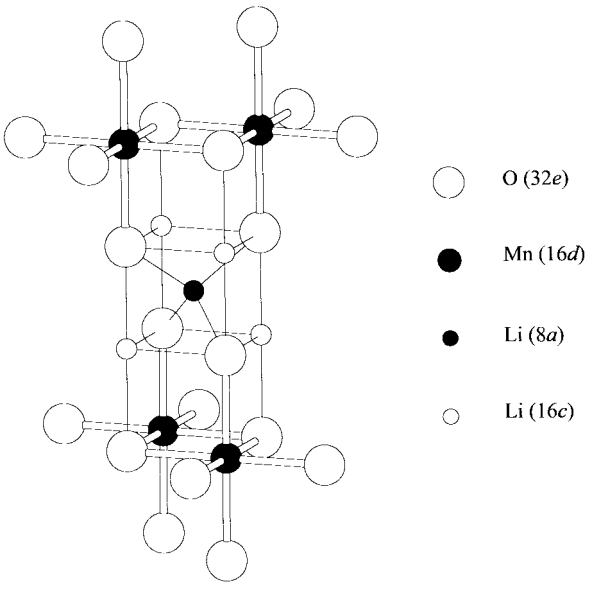

Fig. 1 The coordination in the cubic $LiMn_2O_4$ spinel structure.

Experimental

The spinel powder was synthesised by a solid-state route. A mixture of stoichiometric amounts of $LiOH{\cdot}H_2O$ and manganese(III) acetate (Li/Mn ratio 0.75) was dissolved under stirring in a small amount of hot water. This precursor material was calcined at 600 °C for 10 h and allowed to cool to ambient temperature in air.[9] Phase identification and evaluation of the lattice parameter for the resulting sample were carried out using X-ray and neutron powder diffraction techniques. The X-ray powder data was obtained using a STOE & CIE GmbH STADI position-sensitive detector (PSD) diffractometer with strictly monochromatic Cu-Kα_1-radiation in the 2θ range 10–90°. Neutron powder diffraction data were collected at the Swedish medium-flux steady-state research reactor R2 in Studsvik. A monochromator system was used involving two parallel copper crystals (220-reflection) to give a wavelength of $\lambda = 1.47$ Å. The sample was contained in a vanadium can, and data collected in the 2θ range 9.4–128.0°.

Structure refinement

Rietveld refinement of the cubic $Li_{1+x}Mn_{2-x}O_4$ structure (space group: *Fd*3*m*) was made using the program FULLPROF[10,11] in a two-phase refinement mode involving the monoclinic impurity phase Li_2MnO_3 (space group: *C*2/*m*). The powder diffraction profile used in the refinement covered the 2θ range 15.0–128.0°. The neutron scattering lengths used

were Li: −1.90, Mn: −3.73 and O: 5.803 fm. The diffraction peaks were described by a pseudo-Voigt function; a Lorentzian contribution to a Gaussian peak-shape was refined. A peak-asymmetry correction was made for peaks below 45° in 2θ. The angular dependence of the linewidths was expressed by $H^2 = U\tan^2\theta + V\tan\theta + W$, where H is the full-width at half

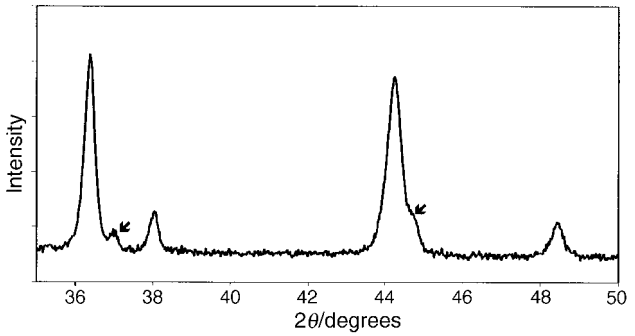

Fig. 2 X-Ray powder diffraction profile. The arrows indicate reflections from the Li_2MnO_3 phase.

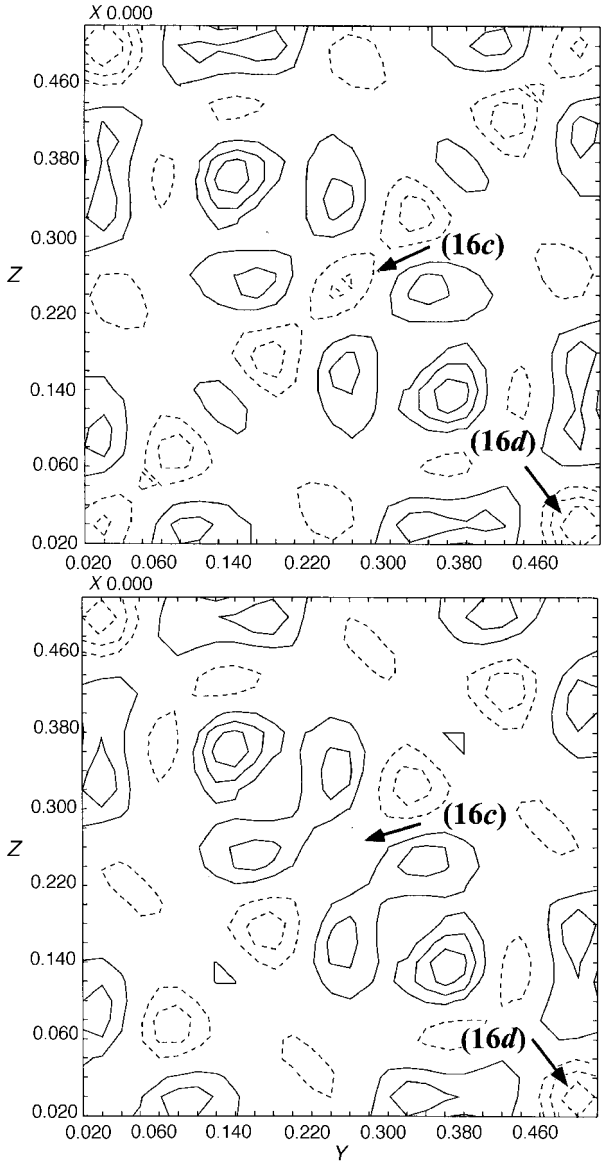

Fig. 3 Contour plots of the Fourier difference calculations for refinement of the extra lithium ions (section at $x = 0.00$ perpendicular to the *ab*-plane; arbitrary interval). (top) 0.25 Li at 16*d*-site; (bottom) 0.14 Li at 16*c*-site.

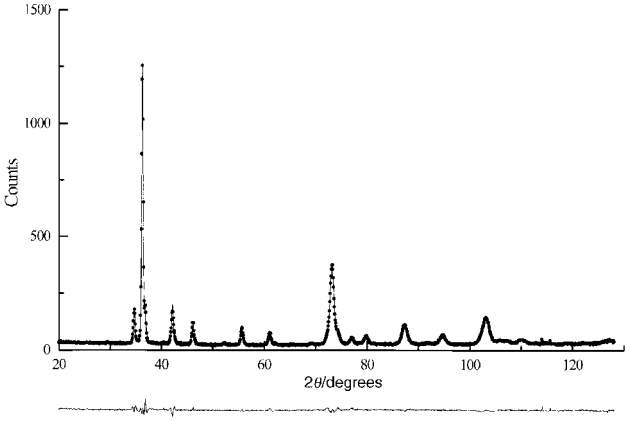

Fig. 4 Observed and calculated neutron diffraction profiles for $Li_{1.14}Mn_{1.86}O_4$ and Li_2MnO_3 (4.8 wt%). The difference between the observed and calculated profiles is also plotted on the same scale.

maximum; U, V and W are refineable parameters. Absorption effects were corrected using the experimentally determined μR value of 0.39 obtained from transmission measurements at $2\theta = 0°$. Background intensities were described by the polynomial expression $y_i = \Sigma B_m[(2\theta_i/90) - 1]^m$, where $0 \leq m \leq 5$. The B_m coefficients for $m = 0$, 1 and 2 were refined, along with one zero-point in 2θ. For each of the two phases, one scale factor was refined. The lattice parameter and the atomic positional parameter for oxygen were refined for the cubic phase. For each crystallographic site, a displacement parameter was refined. The Mn occupation of the octahedral 16*d* site was refined, and the Li/Mn ratio constrained to maintain the stoichiometry $Li_{1+x}Mn_{2-x}O_4$. Atomic positional parameters and displacement parameters for the monoclinic Li_2MnO_3 phase were fixed to values from Strobel & Lambert-Andron.[12] Only the lattice parameters were refined to give: $a = 4.92(1)$ Å, $b = 8.53(1)$ Å, $c = 5.01(1)$ Å, $\beta = 109.5(1)°$, $V = 198.21(1)$ Å^3.

Results and discussion

The sample had been synthesised with a Li/Mn ratio of 0.75 with the aim of producing a stoichiometric lithium-rich spinel, $Li_{1+x}Mn_{2-x}O_4$, $x = 0.28$. Chemical analysis of the resulting powder could confirm a Li/Mn ratio of 0.749(1), but X-ray powder diffraction showed it to contain an impurity phase: monoclinic phase Li_2MnO_3 (space group: $C2/m$) (Fig. 2). From a battery-application point of view, Li_2MnO_3 is a direct source of capacity loss. Lithium extraction from Li_2MnO_3 is precluded since the manganese ions are already Mn^{4+} and therefore cannot be further oxidised. The XRD pattern of cubic $LiMn_2O_4$ and monoclinic Li_2MnO_3 resemble one another closely; their structures are closely related, with the *c*-axis of the monoclinic phase corresponding to the [111]-direction of the cubic phase.

The $Li_{1+x}Mn_{2-x}O_4$ phase could be refined in the cubic space group $Fd3m$, with the refined formulation $Li_{1.25}Mn_{1.75}O_4$ ($R_{Bragg} = 5.62\%$ for 241 reflections and 20 variables). The 'extra' lithium ions were refined in the octahedral 16*d* site; at the manganese site. The amount of the impurity phase (in wt%) can be calculated from:

$$w_j = \frac{s_j Z_j M_j V_j}{\sum_i s_i Z_i M_i V_i}$$

where s_i are the individual scale factors obtained for phase i from the Rietveld refinement, Z_i is the number of formula units per unit cell for phase i, M_i is the mass of the formula unit, and V_i is the unit cell volume.[11] This resulted in 5.3 wt% of Li_2MnO_3. When the amount of the impurity phase and the

Table 1 Refined crystallographic parameters for $Li_{1+x}Mn_{2-x}O_4$ [$x=0.14(1)$] as determined from neutron powder diffraction data[a]

Atom	Position	$x(=y=z)$	B/Å^2	Site occupancy (%)
Li (1)	8*a*	1/8	1.31(2)	100
Li (2)	16*c*	0	0.43(4)	7.0(4)
Mn	16*d*	1/2	0.43(4)	93.0(4)
O	32*e*	0.2637(1)	0.99(3)	100

[a]Space group: *Fd*3*m*; $a=8.1784(6)$ Å, $R_p=6.01\%$, $R_{Bragg}=5.43\%$, $\chi^2=1.31$ for 241 reflections and 20 variables.

refined formula $Li_{1.25}Mn_{1.75}O_4$ were taken into account, a Li/Mn ratio of 0.771(2) was calculated.

From earlier work,[13–15] the lattice parameter is known to decrease linearly with increasing x-value. This is a consequence of the smaller ionic radius of manganese in higher oxidation states. The lattice parameter obtained from the XRD measurement [$a=8.186(1)$ Å] corresponds to an x-value of 0.14(1),[13] which does *not* agree with the refined x-value [0.25(1)]. Moreover, a difference Fourier synthesis [Fig. 3(*a*)] shows a negative peak remaining at the 16*d*-sites ($0\,0\,\frac{1}{2}$), in spite of the fact that this site is already fully occupied by manganese and lithium ions. The negative peaks at ($0\,\frac{1}{4}\,0$), ($0\,\frac{1}{2}\,\frac{1}{4}$), ($0\,0\,\frac{1}{4}$) and ($0\,\frac{1}{4}\,\frac{1}{2}$) relate to oxygen atoms at 32*e*-sites.

In an attempt to rectify these apparent discrepancies in the model, different sites for the extra lithium ions were considered: the tetrahedral 8*b* and 48*f* sites and the octahedral 16*c* site. However, the tetrahedral sites are not possible for lithium ions because of the close distances to the manganese atoms (1.77 Å). The extra lithium ions were refined in the octahedral 16*c* site, and the Rietveld fit is shown in Fig. 4. The difference Fourier now became 'empty' [Fig. 3(*b*)] at the 16*c* site; however, the negative peak at 16*d* site still remained. The parameters obtained from this new Rietveld refinement are given in Table 1, and the refined x-value was 0.14(1) ($R_{Bragg}=5.43\%$ for 241 reflections and 20 variables). This value is now in agreement with the relationship between the lattice parameter and x-value obtained by Gummow *et al.*[13] The refined amount of the Li_2MnO_3 impurity phase was now 4.8 wt% and the Li/Mn ratio became 0.766(2).

The structure of $Li_{1+x}Mn_{2-x}O_4$ has earlier been refined from XRD and ND data for $x=0.27$ and 0.33.[16,17] In both studies, the extra lithium was shown to occupy the 16*d*- and *not* the 16*c*-site. A possible explanation for this can be the different conditions of synthesis; the firing temperature was here 600 °C, compared to 400 °C[16] and 700 °C[17] in earlier work. Moreover, in ref. 17, the starting material involved Mn^{2+} ions in $Mn(NO_3)_2$, while ref. 16 used Mn^{4+} ions in γ-MnO_2. Here, the source of manganese was Mn^{3+} ions in $Mn(CH_3COO)_3{\cdot}2H_2O$. It is also clear that the nature of the starting material determines the incidence of the Li_2MnO_3 impurity: no impurity phase was observed in ref. 16; while <5 wt% Li_2MnO_3 was observed in ref. 17. It would seem that a starting material involving Mn^{3+} ions has a tendency to form the Li_2MnO_3 impurity, as well as resulting in a different Li distribution.

Conclusions

Refinement of a two-phase mixture of $Li_{1+x}Mn_{2-x}O_4$ and Li_2MnO_3, as synthesised from $LiOH{\cdot}H_2O$ and Mn(III) acetate, has resulted in an effective formulation $Li_{1.14}Mn_{1.86}O_4$, with the 'extra' 0.14(1) lithium ions occupying the octahedral 16*c*-sites, and thus *not* replacing the manganese ions at the 16*d*-site as has earlier been reported. It would appear that the precise nature of the $Li_{1+x}Mn_{2-x}O_4$ structure is a sensitive function of the starting materials and the synthesis parameters used.

Acknowledgements

This work has been supported by grants from The Swedish Natural Science Research Council (NFR), The Swedish Board for Technical Development (NUTEK) and the EEC (Joule III) Programme. All are hereby gratefully acknowledged. We are also indebted to H. Rundlöf for his skilled assistance during the neutron data collection.

References

1 M. M. Thackeray, A. de Kock, M. H. Rossouw, D. Liles, R. Bittihn and D. Hoge, *J. Electrochem. Soc.*, 1992, **139**, 363.
2 B. Zachau-Christiansen, K. West, T. Jacobsen and S. Atlung, *Solid State Ionics*, 1990, **40/41**, 580.
3 M. M. Thackeray, W. I. F. David, P. G. Bruce and J. B. Goodenough, *Mater. Res. Bull.*, 1983, **18**, 461.
4 T. Ohzuku, M. Kitagawa and T. Hirai, *J. Electrochem. Soc.*, 1990, **137**, 769.
5 G. Pistoia, D. Zane and Y. Zhang, *J. Electrochem. Soc.*, 1995, **142**, 2551.
6 J. M. Tarascon, W. R. McKinnon, F. Coowar, T. N. Bowmer, G. Amatucci and D. Guyomard, *J. Electrochem. Soc.*, 1994, **141**, 1421.
7 J. C. Hunter, *J. Solid State Chem.*, 1981, **39**, 142.
8 Y. Gao, M. N. Richard and J. R. Dahn, *J. Appl. Phys.*, 1996, **80**, 4141.
9 I. Chen, X. Huang, E. Kelder and J. Schoonman, *Solid State Ionics*, 1995, **76**, 91.
10 H. M. Rietveld, *J. Appl. Crystallogr.*, 1969, **2**, 7.
11 J. Rodriguez-Carvajal, *ILL Internal Report*, FULLPROF computer program.
12 P. Strobel and B. Lambert-Andron, *J. Solid State Chem.*, 1988, **75**, 90.
13 R. J. Gummow, A. de Kock and M. M. Thackeray; *Solid State Ionics*, 1994, **69**, 59.
14 Y. Gao and J. R. Dahn, *J. Electrochem. Soc.*, 1996, **143**, 100.
15 P. Endres, B. Fuchs, S. Kemmler-Sack, K. Brandt, G. Faust-Becker and H. W. Praas, *Solid State Ionics*, 1996, **89**, 221.
16 B. Ammundsen, D. J. Jones, J. Rozière, H. Berg, R. Tellgren and J. O. Thomas, *Chem. Mater.*, 1998, **10**, 1680.
17 T. Takada, H. Hayakawa, E. Akiba, F. Izumi and B. C. Chakoumakos, *J. Solid State Chem.*, 1997, **130**, 74.

Paper 8/04851G